



HAL
open science

Investigation of Mn-Fe magnetic interaction in mechanically alloyed Fe doped-MnAlC by ^{57}Fe Mössbauer spectrometry

Van Tang Nguyen, Frédéric Mazaleyrat, Nirina Randrianantoandro

► To cite this version:

Van Tang Nguyen, Frédéric Mazaleyrat, Nirina Randrianantoandro. Investigation of Mn-Fe magnetic interaction in mechanically alloyed Fe doped-MnAlC by ^{57}Fe Mössbauer spectrometry. *Journal of Magnetism and Magnetic Materials*, 2023, 568, pp.1-9. 10.1016/j.jmmm.2023.170437 . hal-04164841

HAL Id: hal-04164841

<https://cnam.hal.science/hal-04164841>

Submitted on 15 Nov 2023

HAL is a multi-disciplinary open access archive for the deposit and dissemination of scientific research documents, whether they are published or not. The documents may come from teaching and research institutions in France or abroad, or from public or private research centers.

L'archive ouverte pluridisciplinaire **HAL**, est destinée au dépôt et à la diffusion de documents scientifiques de niveau recherche, publiés ou non, émanant des établissements d'enseignement et de recherche français ou étrangers, des laboratoires publics ou privés.

Copyright

Investigation of Mn-Fe magnetic interaction in mechanically alloyed Fe doped-MnAlC by ^{57}Fe Mössbauer spectrometry

Van Tang Nguyen^{1,2}, Frédéric Mazaleyra³, Nirina Randrianantoandro⁴

¹Graduate University of Science and Technology, Vietnam Academy of Science and Technology
18 Hoang Quoc Viet, Cau Giay, Hanoi, Vietnam

²University of Science and Technology of Hanoi, Vietnam Academy of Science and Technology, 18
Hoang Quoc Viet, Cau Giay, Hanoi, Vietnam

³SATIE, ENS Paris-Saclay, 4 avenue des Sciences, 91190 Gif-sur-Yvette, France

⁴Institut des Molécules et Matériaux du Mans – UMR CNRS n°6283, Le Mans Université, Avenue
Olivier Messiaen, 72085 LE MANS Cedex 9

Abstract

Four samples $\gamma_2\text{-Mn}_{40}\text{Fe}_{0.5}\text{Al}_{59.5}$, $\beta\text{-Mn}_{60}\text{Fe}_{0.5}\text{Al}_{39.5}$, and $\varepsilon\text{-Mn}_{50.5}\text{Fe}_{0.5}\text{Al}_{47}\text{C}_2$, $\tau\text{-Mn}_{50.5}\text{Fe}_{0.5}\text{Al}_{47}\text{C}_2$ were synthesized by mechanical alloying method. X-ray diffraction results showed high purity of the γ_2 , β , ε , and τ phases in each sample. Mössbauer measurement at room temperature showed non-ferromagnetic characteristic of the $\gamma_2\text{-Mn}_{40}\text{Fe}_{0.5}\text{Al}_{59.5}$, $\beta\text{-Mn}_{60}\text{Fe}_{0.5}\text{Al}_{39.5}$, and $\varepsilon\text{-Mn}_{50.5}\text{Fe}_{0.5}\text{Al}_{47}\text{C}_2$. Interestingly, $\tau\text{-Mn}_{50.5}\text{Fe}_{0.5}\text{Al}_{47}\text{C}_2$ showed a complex magnetic hyperfine splitting, indicating magnetic ordered structure. The hyperfine interaction in $\tau\text{-Mn}_{50.5}\text{Fe}_{0.5}\text{Al}_{47}\text{C}_2$ was found dependent with temperature, in which isomer shift (IS) and magnetic hyperfine field (B_{hf}) decreased with increasing temperature. The Curie temperature (T_c) was identified to lie between 548 K and 573 K. In order to investigate the magnetic interaction between Fe and Mn atoms in $\tau\text{-Mn}_{50.5}\text{Fe}_{0.5}\text{Al}_{47}\text{C}_2$, local magnetic order of $\tau\text{-Mn}_{50.5}\text{Fe}_{0.5}\text{Al}_{47}\text{C}_2$ was probed by using in-field ^{57}Fe Mössbauer spectrometry. The results showed that Fe and Mn formed a non-collinear magnetic structure with magnetic moments of Fe at different sites showing different canting angles with neighboring Mn atoms.

Keywords: **Mechanical alloy, MnAlFeC, Mössbauer spectrometry, Magnetic interaction.**

Corresponding author: Van Tang Nguyen

Email address: nguyen-van.tang@usth.edu.vn

1. Introduction

Searching for a free rare earth magnet that is able to meet the industrial requirement has been always a need since the crisis of rare earth elements [1]. Among potential candidates, τ -MnAl(C) (crystal system: tetragonal, space group: P4/mmm) is very promising as the $|BH|_{\max}$ could reach 112 kAm⁻³ and the constituents have a very reasonable price. Addition of carbon (C) is well known to prevent τ -MnAl to decompose into β (crystal system: cubic, space group: P4132) and γ_2 (crystal system: Rhombohedral, space group: R3m) [2]. τ -MnAl(C) is often synthesized by heat treatment from high temperature ε -MnAl(C) precursor (crystal system: hexagonal, space group: P63/mmc) at moderate temperature from 400 – 600 °C [3].

However, in τ -MnAl(C) crystal structure, like other tetragonal magnetic materials, there is a non-magnetic layer of Al atoms at 1d site, that does not contribute to its overall magnetic performance, and around 4 at.% of Mn atoms that enter the 1d site, having antiferromagnetic interaction with Mn atoms in the surrounding of the 1a sites [4]. Effort has been done to replace that layer by 3d transition metals in order to improve the magnetization of τ -MnAl(C) [5-7]. In our previous work, doping Fe into τ -MnAl(C) was carried out in order to investigate the influence of Fe addition on the crystallography and magnetic properties of mechanical alloyed τ -MnAlC [4]. Although the magnetic performance was not improved, enhancement in thermal stability of bulk τ -MnAlC was obtained [4], which is beneficial for application of magnetic materials. The reason for the decline of magnetization was attributed to the reduction of its lattice parameters as the distance between neighboring Mn atoms greatly affects their magnetic interaction according to Bethe Slater curve [8]. However, as mentioned in our previous report [4], the Fe atom has its own magnetic moment and how it interacts with Mn atoms also contribute to the overall magnetic properties of the material. So far, only one theoretical study was carried out by Manchanda *et al.* based on density functional theory (DFT). It was reported that doping Fe deteriorates the saturation magnetization of τ -MnAl due to dilution effect that Mn (2.45 μ_B) possesses higher magnetic moment than doped Fe (1.9 μ_B), and/or antiferromagnetic intralayer exchange coupling in the crystal structure [9, 10]. Thus, an experimental investigation of the magnetic interaction between Mn and Fe in Fe doped τ -MnAlC is necessary. Among experimental local magnetic order investigating methods, ⁵⁷Fe Mössbauer spectrometry is a powerful method thanks to its ability to detect a tiny change in hyperfine interaction of probed nuclei and their local environment [11].

Therefore, in this paper, we present an investigation of the magnetic interaction between Fe and Mn in mechanically synthesized Fe-doped MnAlC alloys by employing in-field ^{57}Fe Mössbauer spectrometry. In our previous work, as the ϵ , β and γ_2 could still exist in τ -MnFeAlC, so in order to support the Mössbauer results of τ -MnFeAlC, the ϵ , β , and γ_2 phases were also synthesized and investigated.

2. Materials and Methods

In order to prepare samples for Mössbauer measurements, four samples of the β - $\text{Mn}_{60}\text{Fe}_{0.5}\text{Al}_{39.5}$, and γ_2 - $\text{Mn}_{40}\text{Fe}_{0.5}\text{Al}_{59.5}$, ϵ - $\text{Mn}_{50.5}\text{Fe}_{0.5}\text{Al}_{47}\text{C}_2$, τ - $\text{Mn}_{50.5}\text{Fe}_{0.5}\text{Al}_{47}\text{C}_2$ were synthesized by mechanical alloying method. The β and γ_2 are different in composition because it is easy to get high purity at those compositions. One can find the procedure of mechanical alloying method to make the ϵ and τ - $\text{Mn}_{50.5}\text{Fe}_{0.5}\text{Al}_{47}\text{C}_2$ phases in [4]. The τ - $\text{Mn}_{50.5}\text{Fe}_{0.5}\text{Al}_{47}\text{C}_2$ was achieved by secondary heat treatment at 525 °C for 50 minutes of the ϵ - $\text{Mn}_{50.5}\text{Fe}_{0.5}\text{Al}_{47}\text{C}_2$. The milling conditions of the two samples γ_2 - $\text{Mn}_{40}\text{Fe}_{0.5}\text{Al}_{59.5}$, and β - $\text{Mn}_{60}\text{Fe}_{0.5}\text{Al}_{39.5}$ were the same, but the as-milled powder sealed in a quartz tube under 10^{-4} Torr was annealed at 800 °C for 1h and quenched in water. Since the natural abundance of ^{57}Fe is 2%, the content of the ^{57}Fe in these four samples is not enough to have a good signal and fast recording of Mössbauer spectrometry. Therefore, when weighing the amount of Fe dopant, the ^{56}Fe was mixed with additional ^{57}Fe in all samples. The XRD diagram of those four samples γ_2 - $\text{Mn}_{40}\text{Fe}_{0.5}\text{Al}_{59.5}$, β - $\text{Mn}_{60}\text{Fe}_{0.5}\text{Al}_{39.5}$, ϵ - $\text{Mn}_{50.5}\text{Fe}_{0.5}\text{Al}_{47}\text{C}_2$, and τ - $\text{Mn}_{50.5}\text{Fe}_{0.5}\text{Al}_{47}\text{C}_2$, was characterized by PANalytical – X ray Diffractometer using CuK_α radiation.

^{57}Fe Mössbauer measurements were conducted at different temperatures in zero external magnetic field and under external magnetic field of 8 T at 10 K using a standard transmission geometry equipped with a conventional constant acceleration spectrometer and a ^{57}Fe source diffused into a rhodium matrix. Isomer shift (IS) values are given based on α -Fe at room temperature. In case of measurement with temperature, the samples either were kept inside a cryostat with a plastic sample holder or a cryofurnace with a thin aluminum foil sample holder.

3. Results and Discussion

3.1. Crystallography

Figure 1 shows the XRD diagrams of four synthesized samples and γ_2 - $\text{Mn}_{40}\text{Fe}_{0.5}\text{Al}_{59.5}$, β - $\text{Mn}_{60}\text{Fe}_{0.5}\text{Al}_{39.5}$, ε - $\text{Mn}_{50.5}\text{Fe}_{0.5}\text{Al}_{47}\text{C}_2$, and τ - $\text{Mn}_{50.5}\text{Fe}_{0.5}\text{Al}_{47}\text{C}_2$. Phase identification was carried out using HighScore Plus Software [12]. It is noted that the four phases γ_2 , β , ε , and τ in the four XRD diagrams was obtained with high purity. In detail, for γ_2 - $\text{Mn}_{40}\text{Fe}_{0.5}\text{Al}_{59.5}$, no other phase was detected, while in β - $\text{Mn}_{60}\text{Fe}_{0.5}\text{Al}_{39.5}$, a small amount of MnAlC_3 was identified. In the XRD pattern of ε - $\text{Mn}_{50.5}\text{Fe}_{0.5}\text{Al}_{47}\text{C}_2$ a small amount of Al_2O_3 was detectable that was due to oxidation that may occur during the ball milling and heat treatment processes. High purity of τ - $\text{Mn}_{50.5}\text{Fe}_{0.5}\text{Al}_{47}\text{C}_2$ up to 98%, which was qualified by MAUD program through Rietveld refinement [13], was obtained. This high purity of the τ phase is similar with result achieved in our previous report [4]. A small quantity of Al_2O_3 came from the precursor ε phase as τ - $\text{Mn}_{50.5}\text{Fe}_{0.5}\text{Al}_{47}\text{C}_2$ remained after heat treatment of the ε phase at lower temperature (525 °C for 50 minutes). Other small amount of non-magnetic phases such as β and γ_2 was detected also, as the τ - $\text{MnAl}(\text{C})$ phase is metastable and can decompose into the β and γ_2 phases [14]. It is emphasized that high purity of the phases obtained are very important for Mössbauer measurements since it can reduce effect of impurity phases on the result.

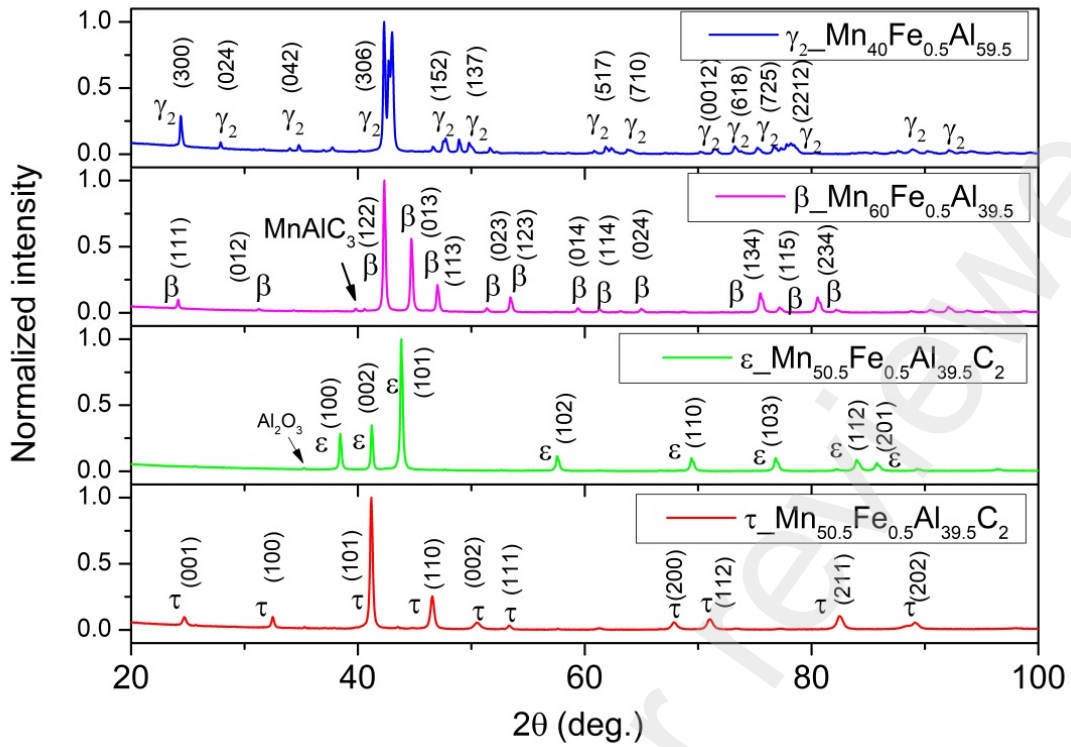


Figure 1. XRD diagrams of investigated samples.

3.2. Mössbauer measurement results

a) Room temperature measurement

Figure 2 depicts the ^{57}Fe Mössbauer spectra recorded at room temperature on $\gamma_2\text{-Mn}_{40}\text{Fe}_{0.5}\text{Al}_{59.5}$, $\varepsilon\text{-Mn}_{50.5}\text{Fe}_{0.5}\text{Al}_{39.5}\text{C}_2$, $\tau\text{-Mn}_{50.5}\text{Fe}_{0.5}\text{Al}_{39.5}\text{C}_2$, and $\beta\text{-Mn}_{60}\text{Fe}_{0.5}\text{Al}_{39.5}$. The hyperfine parameters were refined by using MOSFIT software, a Lorentzian line-fitting program (unpublished Mosfit Program, Le Mans University, France, in 1984). The bubble lines are the raw experimental data and the solid lines are simulated spectra and spectral components as a result of curve fitting process. The quantitative refined values of hyperfine parameters are listed in Table 1.

It is well established that γ_2 , $\beta\text{-MnAl}$ alloys are non-magnetic at room temperature, and the ε phase is believed to be antiferromagnetic below $T_N = 97\text{ K}$ [15], which means ε is paramagnetic at room temperature. As expected, the Mössbauer spectra of $\gamma_2\text{-Mn}_{40}\text{Fe}_{0.5}\text{Al}_{59.5}$, $\varepsilon\text{-Mn}_{50.5}\text{Fe}_{0.5}\text{Al}_{39.5}\text{C}_2$, and $\beta\text{-Mn}_{60}\text{Fe}_{0.5}\text{Al}_{39.5}$ exhibit a quadrupole splitting structure requiring at least two spectral components to be well described (Figure 2). It indicates that at least two sites of Fe in the $\gamma_2\text{-Mn}_{40}\text{Fe}_{0.5}\text{Al}_{59.5}$, $\varepsilon\text{-Mn}_{50.5}\text{Fe}_{0.5}\text{Al}_{39.5}\text{C}_2$, and $\beta\text{-Mn}_{60}\text{Fe}_{0.5}\text{Al}_{39.5}$ that contribute to the total Mössbauer spectra. The two spectral components of $\varepsilon\text{-Mn}_{50.5}\text{Fe}_{0.5}\text{Al}_{39.5}\text{C}_2$ is reasonable with two atoms per unit cell at 2c site of the ε phase

[16]. For the γ_2 -phase that has three sites 18c, 9b and 3a with 88 atoms per unit cell, and the β -phase that has two sites 12d and 8c with 20 atoms per unit cell [16], there may be more Fe sites that add up to the total spectra; however, it is not easy to consider all minor contributions. Demonstration of the unit cells of the four phases is provided in the supplementary material.

Table 1. Refinement parameters of γ_2 -Mn₄₀Fe_{0.5}Al_{59.5}, β -Mn₆₀Fe_{0.5}Al_{39.5}, ε -Mn_{50.5}Fe_{0.5}Al₄₇C₂, and τ -Mn_{50.5}Fe_{0.5}Al₄₇C₂ spectra at room temperature.

Phase	Spectral Component	IS (mm/s) (± 0.01)	QS/2 ε (mm/s) (± 0.01)	B _{hf} (T) (± 1)	Content (%) (± 1)
γ_2 -Mn ₄₀ Fe _{0.5} Al _{59.5}	1	0.28	0.17	0	44
	2	0.29	0.64	0	56
β -Mn ₆₀ Fe _{0.5} Al _{39.5}	1	0.18	0.31	0	77
	2	0.29	0.58	0	23
ε -Mn _{50.5} Fe _{0.5} Al ₄₇ C ₂	1	0.23	0.52	0	30
	2	0.23	0.24	0	70
τ -Mn _{50.5} Fe _{0.5} Al ₄₇ C ₂	1	0.27	0.24	14	53
	2	0.24	0.25	11	27
	3	0.31	0.05	7	13
	4	0.15	0.59	0	7

IS: Isomer shift
 QS/2 ε : quadrupole shift
 B_{hf}: Magnetic hyperfine field

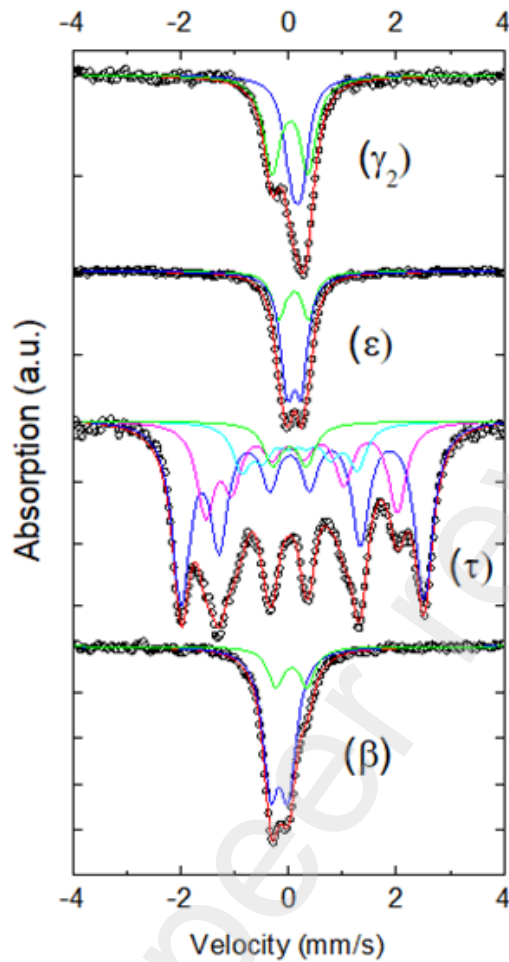


Figure 2. Mössbauer measurement of γ_2 -Mn₄₀Fe_{0.5}Al_{59.5}, β -Mn₆₀Fe_{0.5}Al_{39.5}, ϵ -Mn_{50.5}Fe_{0.5}Al₄₇C₂, and τ -Mn_{50.5}Fe_{0.5}Al₄₇C₂ at room temperature

Interestingly, the τ -Mn_{50.5}Fe_{0.5}Al₄₇C₂ spectrum demonstrates a complex magnetic hyperfine splitting with broad lines, signaling the presence of a distribution of atomic sites occupied by iron atoms. In this case, several refinement models can be implemented to reproduce the shape of the experimental spectrum, such as the use of a sextuplet distribution with discrete values of hyperfine fields. The best fit model was obtained with four spectral components, in which three spectral components has sextet structure and one with doublet. The sextet structure resulted from magnetic hyperfine field (B_{hf}) splitting indicates magnetic interaction of Fe atoms with the surrounding atoms. It is noted that while the IS values of the three magnetic spectral components of τ -Mn_{50.5}Fe_{0.5}Al₄₇C₂ are comparable with that of γ_2 -Mn₄₀Fe_{0.5}Al_{59.5}, ϵ -Mn_{50.5}Fe_{0.5}Al₄₇C₂, and β -Mn₆₀Fe_{0.5}Al_{39.5}, the quadrupole shift (2ϵ) values noticeably smaller. This could come from the fact that the τ phase is close to body centered cubic with an extended c lattice parameter, and the magnitude of 2ϵ depends on the asymmetry of the charge distribution that surrounds the ^{57}Fe atomic nucleus, which is

smallest for surrounding charge distribution in cubic symmetry. If one examines the sites of Fe that contribute to the four spectral components, one can consider that since there are two inequivalent positions 1a (0; 0; 0) and 1d (1/2;1/2;1/2) sites in tetragonal τ -MnAl(C) phase, Fe atoms are supposed to substitute in these two positions. The empirical atomic radius of Fe (126 pm) is closer to that of Mn (127 pm) rather than Al (143 pm) [17]; therefore, it is reasonable that Fe would preferentially substitute Mn. Considering the content of each spectral component in Table 1, the first spectral component, which accounts for 53%, is attributed to Mn (1a), and the second to Al (1d) site, which accounts for 27%. It is noted that the B_{hf} at 1a (0; 0; 0) site is higher than at the 1d (1/2; 1/2; 1/2) site, which could originate from the difference in interatomic distances between Fe and the neighboring Mn at each site. Indeed, according to the Bethe-Slater curve, especially for the case of Mn, magnetic coupling strongly depends on the interatomic distance [8].

The third spectral component has a relatively smaller B_{hf} which can be attributed to Fe sites with a smaller number of neighboring Mn atoms contributing to the B_{hf} . Therefore, these Fe sites may lie at the surface of crystallite. In addition, as studied by C. Yanar *et al.*, the structure of τ phase is characterized by numerous lattice defects including dislocations, antiphase boundaries, and twins [18]. Hence, Fe sites of the third spectral component may also come from the edge of the lattice defects.

The fourth spectral component that accounts for 7 % of the doped ^{57}Fe is a non-magnetic ordering spectral component. One can notice that its high 2ε is similar to other non-magnetic spectral components of ε , γ_2 , and β phases. Therefore, the fourth spectral component could be assigned to existing ε , γ_2 , and β phases in $\tau\text{-Mn}_{50.5}\text{Fe}_{0.5}\text{Al}_{47}\text{C}_2$. Other possibilities could come from Fe sites at the grain boundary.

b) Temperature dependence measurement

Since there is magnetic hyperfine field interaction of Fe with the neighboring atoms in $\tau\text{-Mn}_{50.5}\text{Fe}_{0.5}\text{Al}_{47}\text{C}_2$, it is interesting to investigate how the interaction is affected by temperature. Therefore, Mössbauer measurement of $\tau\text{-Mn}_{50.5}\text{Fe}_{0.5}\text{Al}_{47}\text{C}_2$ at different temperatures was also carried out, and the result was depicted in Figure 3. The refined values of B_{hf} and IS of these spectra was plotted in Figure 4 and Figure 5, respectively.

One can notice that as the temperature of measurement increased, the average value of hyperfine field B_{hf} is reduced, (Figure 4), accompanying with change in the spectra structure. In detail, as the temperature reached 573 K, the magnetic hyperfine splitting

disappeared and only 2ε and IS remained in the spectrum. In fact, the measurement is also a method to identify the T_c of magnetic materials. From above analysis, the T_c is believed to lie between 548K and 573K, where the B_{hf} becomes negligible. The T_c determined by Mössbauer measurement is in agreement with the result (in range of 560 K) measured for τ - $Mn_{51}Al_{47}C_2$ and τ - $Mn_{49}Fe_2Al_{47}C_2$ by thermomagnetic method in our previous report [4].

Figure 5 shows that the value of IS decreased when the temperature increased, similar to behavior of B_{hf} . Indeed, in Mössbauer spectrometry, the value of IS corresponds to the position of the barycenter of the spectrum with respect to the origin of the velocity range. Its temperature dependence, linked to a relativistic effect, so-called the second-order Doppler effect, leads to the dynamic properties of crystal lattices, especially the local vibration modes for defects and impurities. Using the Debye model for the phonon spectrum, the temperature dependence of the isomer shift is given by the following equation[19]:

$$IS(T) = IS(0) - \frac{3k_B T}{2mc} \left[\frac{3\theta_D}{8T} + 3 \left(\frac{T}{\theta_D} \right)^3 \int_0^{\theta_D/T} \frac{x^3}{e^x - 1} dx \right] \quad (1)$$

where m is the mass of the ^{57}Fe nucleus, k_B is the Boltzmann constant, c is the speed of light and θ_D is the Debye Temperature. The first term $IS(0)$ is composition dependent, while the second corresponds to the second-order Doppler shift, which is exclusively dependent on the temperature. According to this equation, the isomer shift value decreases when the temperature increases.

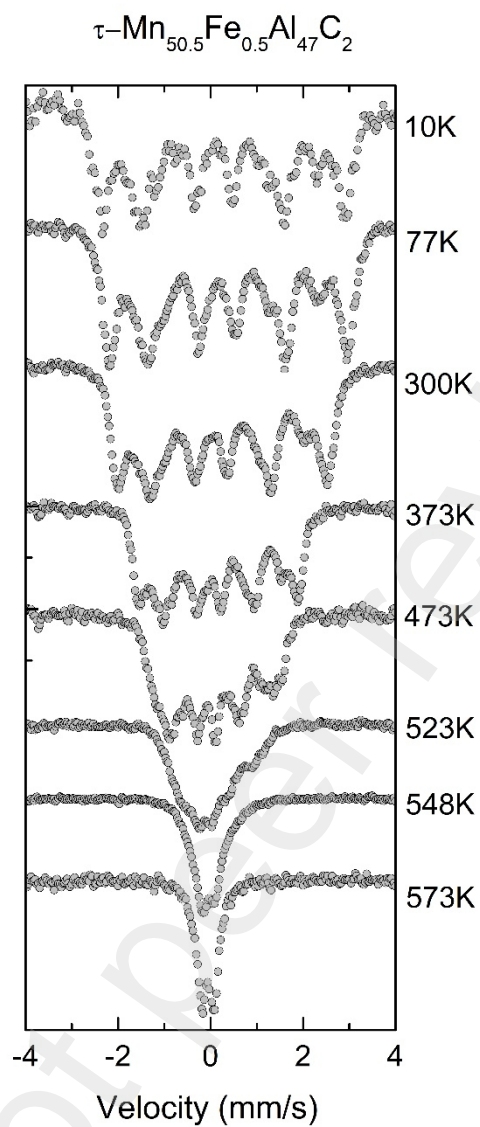


Figure 3. Mössbauer spectra of $\tau\text{-Mn}_{50.5}\text{Fe}_{0.5}\text{Al}_{47}\text{C}_2$ at different temperatures.

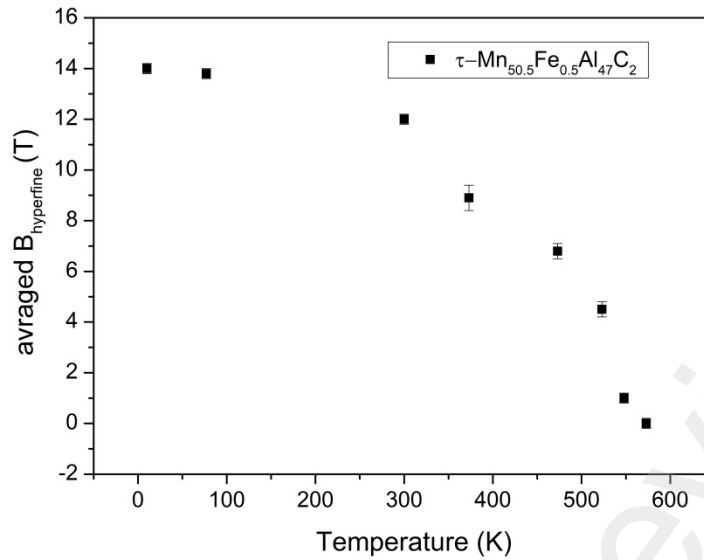


Figure 4. B_{hf} of $\tau\text{-Mn}_{50.5}\text{Fe}_{0.5}\text{Al}_{47}\text{C}_2$ at different temperatures.

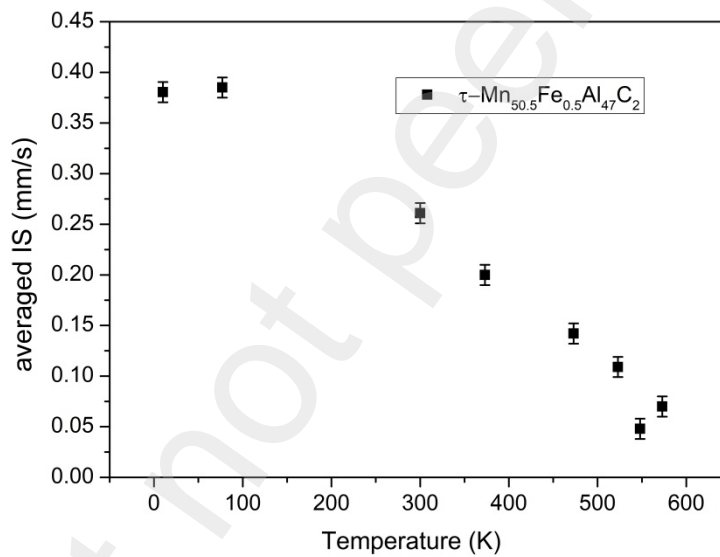


Figure 5. IS of $\tau\text{-Mn}_{50.5}\text{Fe}_{0.5}\text{Al}_{47}\text{C}_2$ at different temperatures.

c) In-field measurement

In order to investigate magnetic interactions between Fe and Mn, in-field (under application of external magnetic field of 8T) Mössbauer measurement of $\tau\text{-Mn}_{50.5}\text{Fe}_{0.5}\text{Al}_{47}\text{C}_2$ was carried out at 10 K and the results are depicted with the zero-field $\tau\text{-Mn}_{50.5}\text{Fe}_{0.5}\text{Al}_{47}\text{C}_2$ at the same temperature in Figure 6. The experimental spectrum at zero magnetic field at 10 K can still be well fitted by 4 spectral components as it was done at room temperature. The higher value of B_{hf} (Table 2) compared to the room temperature

values was expected since at lower temperature the magnetic ordering is strengthened due to lower thermal agitation. Four spectral components were also used to fit the in-field Mössbauer spectrum, which is in agreement with the used zero-field fitting model (Figure 6).

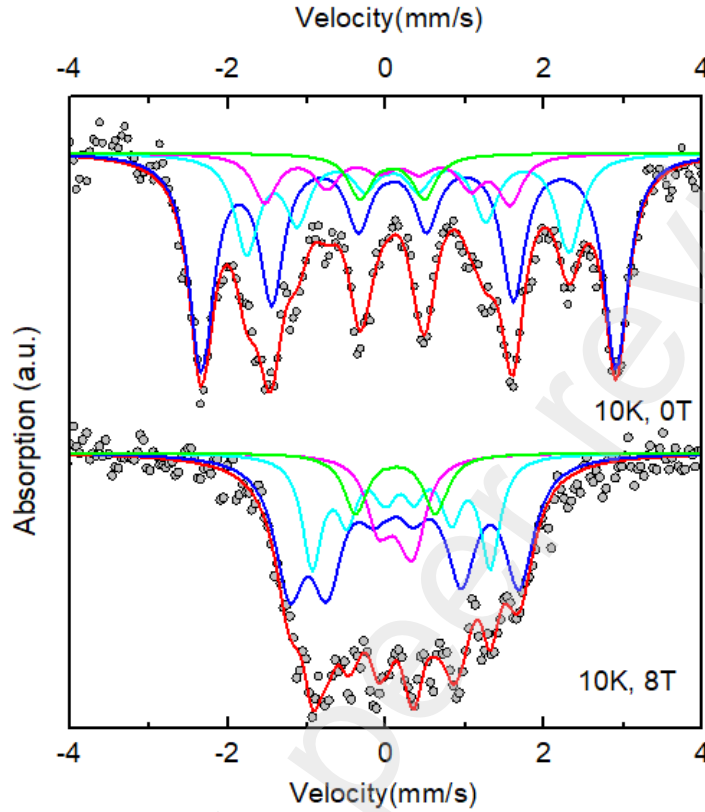


Figure 6. ^{57}Fe Mössbauer spectra of $\tau\text{-Mn}_{50.5}\text{Fe}_{0.5}\text{Al}_{47}\text{C}_2$ recorded at 10 K, zero field and in-field $B_{\text{ext}} = 8$ T.

It is important to notice that when an external magnetic field (B_{ext}) is applied, the measured B_{hf} is now the effective hyperfine field B_{eff} [20]:

$$\vec{B}_{\text{eff}} = \vec{B}_{\text{hf}} + \vec{B}_{\text{ext}} \quad (2)$$

or

$$B_{\text{hf}} = \sqrt{B_{\text{eff}}^2 + B_{\text{ext}}^2 - 2B_{\text{eff}}B_{\text{ext}}\cos\beta} \quad (3)$$

where β is the canting angle between the directions of the B_{ext} and the B_{eff} . It is noted that in our experiment the B_{ext} is applied in parallel to the gamma ray (Figure 7a).

In comparison between zero and in-field Mössbauer spectra of $\tau\text{-Mn}_{50.5}\text{Fe}_{0.5}\text{Al}_{47}\text{C}_2$ at 10 K, one can see that mean hyperfine value of in-field Mössbauer spectrum was clearly reduced (Figure 6). Indeed, as shown in Table 2, refined values of B_{eff} of three magnetic spectral components are reduced in comparison of their zero-field values (B_{hf}). According

to the formula (1), B_{hf} of each spectral component has to be in reversed direction with respect to the B_{ext} .

The MOSFIT program used for refining the in-field spectrum allows to obtain the values of the canting angle β , then one can visualize the deviation in direction of B_{hf} with B_{ext} . It is noted that the obtained B_{hf} values (Table 2), which are calculated from B_{eff} based on the formula (2), are close to those found by refinement of zero-field spectrum recorded at the same temperature (10 K) and the content of each spectral component is well reproduced. From Figure 7b, one can see clearly the deviation of B_{hf} with B_{ext} . In addition, in Fe-containing alloys, the B_{hf} is opposite to the Fe magnetic moment [21]. Therefore, values of angle β indicate how the Fe magnetic moments are deviated from the direction of the B_{ext} (Figure 7b). The β values of the first and the second spectral components (Table 2) demonstrate that the applied field of 8 T was not enough to align the magnetic moment of Fe to the direction of the B_{ext} . It is noticed that the deviation of Fe magnetic moment is more pronounced at the first spectral component, corresponding to suggested 1a (0; 0; 0) position, than at the second spectral component, 1d ($\frac{1}{2}$; $\frac{1}{2}$; $\frac{1}{2}$) position. The refined $\beta = 180^\circ$ of the third magnetic spectral component suggests that the Fe magnetic moment is aligned along the applied field. The larger value of β of the third spectral component supports the proposal that it is attributed to Fe sites at surface of crystallite and defects where the Mn content is poor. Indeed, according to the work conducted by L. Pareti *et al.*, it was shown that the anisotropy field of MnAl alloy is lower in regions that is poor in Mn [22]. Besides, the proposal is also in agreement with the fact that the nucleation is often initiated at region close to defects [23].

Moreover, although in the ^{57}Fe in-field measurement of $\tau\text{-Mn}_{50.5}\text{Fe}_{0.5}\text{Al}_{47}\text{C}_2$ only the behavior of Fe magnetic moments was probed, one can recognize the interaction of Mn and Fe by the fact that all magnetic moments present in the sample are also affected by the applied field (B_{ext}). Mn atoms at 1a site (0; 0; 0) are then oriented in the direction of the B_{ext} since Mn atoms at these sites are ferromagnetically coupled. Experimentally, our own investigation of room temperature $M(H)$ curve of $\tau\text{-Mn}_{54.2}\text{Al}_{43.8}\text{C}_2$ demonstrated that saturation magnetization was almost reached under 7 T [2]. A simple two-dimension sketch of $\tau\text{-Mn}_{50.5}\text{Fe}_{0.5}\text{Al}_{47}\text{C}_2$ is illustrated in Figure 8. It means that the Fe magnetic moments do not antiferromagnetically couple with the neighboring Mn atoms as predicted by P. Manchanda *et al* [24], instead the Fe magnetic moments are non-collinear, forming canting

angles whose magnitude depend on its sites, with neighboring Mn magnetic moments (Figure 8). It is, therefore, in addition to the reduction of cell parameters, the calculated smaller magnetic moment of Fe, which was concluded in our previous report [4], the deviation in direction of Fe magnetic moment also contribute to the reduction in magnetization of τ -MnAlC when doping Fe.

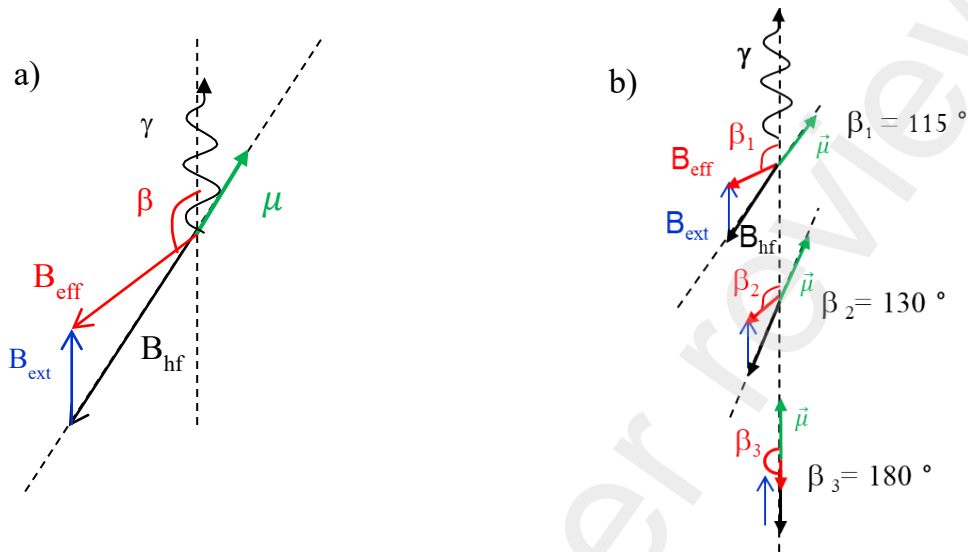


Figure 7. a) Relationship between induction fields vectors (B_{ext} , B_{eff} , B_{hf}), μ is the magnetic moment of Fe.

(b) Demonstration with different values of β showing the deviation of B_{ext} and Fe magnetic moment.

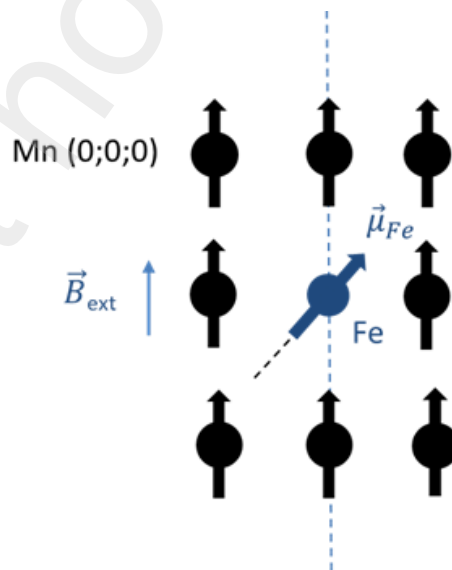


Figure 8. Schematic 2D illustration of Fe and Mn magnetic moments

Table 2. Refinement of hyperfine fields of zero and in-field Mössbauer spectra of τ -Mn_{50.5}Fe_{0.5}Al₄₇C₂ at 10 K

	Spectral component	IS (mm/s) (± 0.01)	QS/2 ϵ (mm/s) (± 0.01)	B_{hf} (T) (± 1)				Content (%) (± 1)
Zero - field	1	0.38	0.24	16				56
	2	0.38	0.20	12				26
	3	0.35	0.08	9				12
	4	0.32	0.79	0				6
	Spectral component	IS (mm/s) (± 0.01)	QS /2 ϵ (mm/s) (± 0.01)	B_{hf} (T) (± 2)	B_{eff} (T) (± 1)	β (°) (± 5)	Content (%) (± 1)	
In-field ($B_{\text{ext}} = 8\text{T}$)	1	0.38	0.14	14	9	115	53	
	2	0.39	0.03	13	7	130	25	
	3	0.39	-0.12	9	1	180	13	
	4	0.33	0.86	0	0	0	9	

4. Conclusions

The γ_2 -Mn₄₀Fe_{0.5}Al_{59.5}, β -Mn₆₀Fe_{0.5}Al_{39.5}, ϵ -Mn_{50.5}Fe_{0.5}Al₄₇C₂, and τ -Mn_{50.5}Fe_{0.5}Al₄₇C₂ were successfully synthesized by mechanical alloying method with high purity.

⁵⁷Fe Mössbauer spectra at room temperature of γ_2 -Mn₄₀Fe_{0.5}Al_{59.5}, β -Mn₆₀Fe_{0.5}Al_{39.5}, ϵ -Mn_{50.5}Fe_{0.5}Al₄₇C₂, and τ -Mn_{50.5}Fe_{0.5}Al₄₇C were recorded. While the γ_2 -Mn₄₀Fe_{0.5}Al_{59.5}, β -Mn₆₀Fe_{0.5}Al_{39.5}, ϵ -Mn_{50.5}Fe_{0.5}Al₄₇C₂ exhibit non ferromagnetic characteristics, magnetic splitting was determined in τ -Mn_{50.5}Fe_{0.5}Al₄₇C₂, which implies magnetic ordered structures. The experimental spectra were well fitted by four spectral components that could belong to sites at 1a, 1d, sites at surface of crystallite, dislocation defects, and sites at remaining ϵ , γ_2 , β or at grain boundaries.

Both IS and B_{hf} of probed Fe in τ -Mn_{50.5}Fe_{0.5}Al₄₇C showed a similar behavior with temperature. In detail, both IS and B_{hf} increased when the temperature decreased. The T_c was identified to lie within 548 K and 573 K.

The interaction between Fe and Mn was clarified by in-field Mössbauer measurement at 10 K and 8 T. It was found that Fe and Mn formed a non-collinear magnetic structure. Fe magnetic moment at different sites showed different canting angles

with neighboring Mn. The non-collinear magnetic structure of Fe and Mn contribute to the reduction in magnetization of τ -MnAlC alloy when adding Fe.

6. Acknowledgment

This work was funded by Graduate University of Science and Technology under grant number GUST.STS. DT2020-KHVL05.

References

- [1] J.M.D. Coey, Permanent magnets: Plugging the gap, *Scripta Materialia*, 67 (2012) 524-529.
- [2] N. Van Tang, F. Calvayrac, A. Bajorek, N. Randrianantoandro, Mechanical alloying and theoretical studies of MnAl (C) magnets, *Journal of Magnetism and Magnetic Materials*, 462 (2018) 96-104.
- [3] H. Kōno, On the Ferromagnetic Phase in Manganese-Aluminum System, *Journal of the Physical Society of Japan*, 13 (1958) 1444-1451.
- [4] V.T. Nguyen, F. Mazaleyrat, F. Calvayrac, Q.M. Ngo, N. Randrianantoandro, Investigation on magnetic properties of mechanically alloyed τ -MnAlC with Fe addition, *Journal of Magnetism and Magnetic Materials*, 546 (2022) 168892.
- [5] L. Feng, K. Nielsch, T.G. Woodcock, Enhanced Thermal Stability of the τ -Phase in MnAl-C Alloys with Ni Additions, *Journal of Alloys and Compounds*, (2021) 159554.
- [6] Z. Xiang, Y. Song, B. Deng, E. Cui, L. Yu, W. Lu, Enhanced formation and improved thermal stability of ferromagnetic τ phase in nanocrystalline Mn55Al45 alloys by Co addition, *Journal of Alloys and Compounds*, 783 (2019) 416-422.
- [7] J. Florian, F. Jens, N. Kornelius, T.G. Woodcock, The Influence of Cu-Additions on the Microstructure, Mechanical and Magnetic Properties of MnAl-C Alloys, *Scientific Reports (Nature Publisher Group)*, 10 (2020).
- [8] B.D. Cullity, C.D. Graham, *Introduction to magnetic materials*, John Wiley & Sons, 2011.
- [9] P. Manchanda, P. Kumar, A. Kashyap, M. Lucis, J.E. Shield, A. Mubarak, J. Goldstein, S. Constantinides, K. Barmak, L. Lewis, Intrinsic Properties of Fe-Substituted L10 Magnets, *IEEE Transactions on Magnetics*, 49 (2013) 5194-5198.
- [10] P. Manchanda, A. Kashyap, J.E. Shield, L. Lewis, R. Skomski, Magnetic properties of Fe-doped MnAl, *Journal of Magnetism and Magnetic Materials*, 365 (2014) 88-92.
- [11] R. Herber, Introduction to Mossbauer spectroscopy, *Journal of Chemical Education*, 42 (1965) 180.
- [12] M.S. T. Degen, E. Bron, U. König, G. Nénert, The HighScore suite, in: *Powder Diffraction December 2014*, pp. S13-S18.
- [13] L. Lutterotti, R. Camprotrini, S. Gialanella, R. Di Maggio, Microstructural Characterisation of Amorphous and Nanocrystalline Structures Through Diffraction Methods, *Materials Science Forum*, 343-346 (2000) 657-664.
- [14] F. Maccari, A. Aubert, S. Ener, E. Bruder, I. Radulov, K. Skokov, O. Gutfleisch, Formation of pure tau-phase in Mn–Al–C by fast annealing using spark plasma sintering, *Journal of Materials Science*, 57 (2022) 6056-6065.
- [15] J.J. Wysocki, P. Pawlik, A. Przybył, Magnetic properties of the non-oriented ϵ -phase in Mn–Al–C permanent magnet, *Materials Chemistry and Physics*, 60 (1999) 211-213.
- [16] H. edited by Theo, *International tables for crystallography. Volume A, Space-group symmetry*, Fifth, revised edition. Dordrecht ; London : Published for the International Union of Crystallography by Kluwer Academic Publishers, 2002., 2002.
- [17] A.F. Wells, *Structural inorganic chemistry*, Oxford university press, 2012.
- [18] C. Yanar, J. Wieszorek, W. Soffa, V. Radmilovic, Massive transformation and the formation of the ferromagnetic L1 0 phase in manganese-aluminum-based alloys, *Metallurgical and Materials Transactions A*, 33 (2002) 2413-2423.
- [19] J. Cieślak, S.M. Dubiel, J. Żukrowski, M. Reissner, W. Steiner, Determination of the Debye temperature of the σ -phase Fe-Cr alloys, *Physical Review B*, 65 (2002) 212301.

- [20] J.-M. Greneche, The contribution of ^{57}Fe Mössbauer spectrometry to investigate magnetic nanomaterials, in: Mössbauer spectroscopy, Springer, 2013, pp. 187-241.
- [21] Q. Samara, A. Al-Sharif, S. Mahmood, On the magnetic properties and hyperfine fields in Fe-containing alloys: A theoretical study, *physica status solidi c*, 3 (2006) 3285-3291.
- [22] L. Pareti, F. Bolzoni, F. Leccabue, A. Ermakov, Magnetic anisotropy of MnAl and MnAlC permanent magnet materials, *Journal of applied physics*, 59 (1986) 3824-3828.
- [23] R. DeBlois, C. Bean, Nucleation of ferromagnetic domains in iron whiskers, *Journal of Applied Physics*, 30 (1959) S225-S226.
- [24] P. Manchanda, P. Kumar, A. Kashyap, M. Lucis, J.E. Shield, A. Mubarak, J. Goldstein, S. Constantinides, K. Barmak, L. Lewis, Intrinsic Properties of Fe-Substituted $L1_0$ Magnets, *IEEE Transactions on Magnetism*, 49 (2013) 5194-5198.